
Article:
Ghaei, A., Khosravi, M., Badrossamay, M. et al. (1 more author) (2017) Micro-dimple rolling operation of metallic surfaces. International Journal of Advanced Manufacturing Technology, 93. pp. 3749-3758. ISSN 0268-3768

https://doi.org/10.1007/s00170-017-0790-3

Micro-Dimple Rolling Operation of Metallic Surfaces

A. Ghaei[a,1],M. Khosravi[a], M. Badrossamay[a], H. Ghadbeigi[b]

[a] *Department of Mechanical Engineering, Isfahan University of Technology, Isfahan, 84156-83111, Iran*

[b] *Department of Mechanical Engineering, The University of Sheffield, UK*

Abstract

The presence of micro-dimples on the surface of workpieces has long been known to have a positive impact on the friction control and wear resistance at the sliding surfaces. Several manufacturing processes have been used to generate micro-dimples on the surfaces of parts subjected to mechanical contact. Among those methods, metal forming based techniques have received little attention in the literature mainly due to the challenges present in formation of sub-millimetre dimples using these processes. In this study, a micro-dimple rolling apparatus was developed to rapidly generate dimples with square cross-sections and side dimensions of smaller than 200 µm. The dimples were formed on the surface of a low carbon structural steel and the effect of generated texture on friction and wear was studied through pin-on-disc test. In comparison with untextured surfaces, the results proved that the dimples formed by the proposed system could effectively reduce the friction coefficient by up to 23% and weight loss due to wear by up to 50%.

Keywords: Surface texturing; micro-dimple; micro-forming; friction; wear.

1. Introduction

Friction plays an important role in mechanical systems. It can play a positive role, e.g. brake systems in automotive applications, or a negative role as a mean to dissipate the productive energy, e.g. in moving parts in an automobile engine, where friction may dissipate up to 40% energy [1]. Therefore, controlling

[1] Corresponding Author. Department of Mechanical Engineering, Isfahan University of Technology, Isfahan, 84156-83111, Iran.
Tel: +98-313-391 5246
Fax: +98-313-391 2628
Email: ghaei@cc.iut.ac.ir

the friction characteristics of contacting surfaces is of prime importance in engineering systems. Surface texturing, in which micro-dimples or micro-channels are intentionally created on the surface, has proven to be an effective method for controlling friction. The use of intentionally created surface irregularities to improve tribological properties was first discussed in the 1960's [2]. Several theoretical and experimental studies have been devoted to surface texturing and its effect on tribological properties of different workpieces such as piston ring [3,4], bearings [5-8], bushings [9,10], mechanical seals [11,12] and even in medical needles [13]. The micro-dimples usually improve the tribological properties through different mechanisms depending on the working conditions. The micro-textures may act as reservoirs for lubricant [14], and thereby decrease lubricant leakage and also lubricate the surfaces for a longer time compared to untextured surface (UTS). It is reported that the build-up pressure in the dimples may increase the film thickness and thus change the lubrication regime from mixed to hydrodynamic lubrication [15]. Zhou et al. [16] reported that the wear debris were trapped into the dimples and reduced the risk of scratching the surfaces during sliding contact. In dry contact conditions where no lubricant is used, the effective contact area is reduced due to the presence of dimples resulting in smaller frictional force compared to UTS [17]. Greiner et al. [18] reported that surface texturing may reduce the friction forces by up to 80% and the smaller dimples are more effective at larger velocity gradients.

Several manufacturing processes have been employed to generate micro-dimples on the workpiece surfaces. The main established techniques include laser ablation [18-21], photochemical machining [22,23], electrochemical machining [24-27] and mechanical micro-machining [28-30]. The selection of an appropriate technique to fabricate dimples is dependent on several parameters such as workpiece material, dimple size, dimple shape, required accuracy and workpiece shape and size. A high energy pulsed laser beam is used in Laser texturing to selectively melt and vaporize the workpiece surface and generate the required pattern. One dimple is generated at a time by the laser beam but the processing times are relatively short as the pulse durations are very short, i.e. microseconds to femtoseconds. This process is considered accurate and can be used for almost all materials. However, expensive equipment is required for laser texturing and the process generates a recast layer on the workpiece surface.. The contacting surfaces are collectively etched using a photoresist resin mask and a chemical etchant in photochemical machining process. The process can be used for mass production but it is not generally an environmentally friendly process as the waste materials and chemicals are hazardous and expensive to dispose. The electrochemical machining removes the workpiece particles using a high current electricity that is passed between the tool and the workpiece through an electrolytic material. Although

formation of defects such as burrs, cracks or heat-affected zones can be prevented upon the selection of proper process parameters, this technique is only applicable for electrically conductive materials. Additionally new masks are also required for each individual workpiece to be textured which adds to the cost and time of the process. In the mechanical micro-machining operation, a miniature cutting tool cuts through the workpiece and removes the unwanted material. The main drawbacks of this process is the need for an expensive micro-milling machine tool and relatively long processing time as only one dimple is created at a time. Other techniques such as deformation-based texturing [16], reactive ion etching [31], ultrasonic nanocrystal surface modification [32], abrasive jet machining [33] and LIGA (Lithography, Electroplating, and Molding) [34] have also been utilized to create surface textures.

Deformation-based techniques could potentially be a better choice for mass production due to inexpensive equipment, low manufacturing cost, environmentally friendly process, without negative side effect and material waste. However, there are several challenges associated with these techniques that need to be addressed. The metal forming systems often generate one dimple at a time, and therefore it is usually time consuming to generate thousands of dimples on a regular workpiece. In addition, as the dimple size decreases, due to the so-called size effect phenomenon, the effects of high sensitivity to backlash in motion mechanisms as well as elastic deflections of tooling because of forming forces on the produced dimples become more prominent. Therefore, tooling systems with closer manufacturing tolerances are required. It is reported that except the deformation-based techniques, other operations are capable to fabricate dimples with diameters of smaller than 50 µm.

According to the available advantages of micro-metal forming, this process could potentially be used for surface texturing in mass production of practical workpieces. Futamura et al. [35] developed a micro-dimple forming tool to generate dimples on the inner wall of pipes to improve the anti-seizing properties of sliding surfaces of mechanical components. They used roller-burnishing process to flatten the bumps formed around the dimples. Zhou et al. [36] developed a micro-forming system to generate micro-channels on the surface of thin sheet metals. Pre-textured rollers were used to create an array of micro-channels through a combination of rolling and indentation actions. Zhou et al. [37] later used the system to study the features of formed micro-channels such as the channel profile and uniformity of its depth. Their measurements showed that channels of approximately 100 µm wide by 15 µm deep were successfully formed on AA5052 aluminium alloy with a nominal thickness of 500 µm.

The purpose of this work is to develop a cost-effective micro-dimple rolling apparatus for high-speed fabrication of micro-dimples on a flat surface. In this context, it is necessary to use relatively simple and

inexpensive equipment and to create several dimples in a short time. The system was mounted on a milling machine to provide the required motions for the tool and hold the workpiece. The effects of generated micro-dimples on wear resistance and frictional contact of the test samples was studied in order to determine the effect of the produced dimples on friction and wear rate of the material under different normal loads, relative sliding velocities and lubrication conditions.

2. Design Procedure

2.1. micro-dimple rolling apparatus

A bespoke experimental setup was designed (Figure 1a) to create dimples using a controlled axial motion of derive axes combined with a free rotational motion of specially designed forming tool (Figure 1b). The designed forming tool consists of indentation teeth resembling a circular saw blade that indents into the surface of the workpiece to create the required dimples with selected parameters including depth, area etc. The workpiece is fixed on a bed that allows in-plane orthogonal displacement while the forming tool is attached to a load actuator in order to provide the required indentation force that is predicted as one of the process parameters using finite element modelling approach. The applied compressive force results in the formation of initial dimples. The table is moved in the longitudinal direction forcing the tool to rotate around its axis while it is compressed on the surface of the workpiece. The tool rotation brings the next tooth into contact with the workpiece generating additional dimples in a row. The forming tool is then moved in the transverse direction with the required pitch size followed by longitudinal motion of the table to create the next row of dimples. The process continues until the whole surface is swept by the tool.

The tool geometry was designed based on the required area density, shape and size of the dimples. In this study, the forming tool was designed assuming that the dimple shape was a square pyramid with a vertex angle equal to the Vickers indenter tip, i.e. 136°. Table 1 shows the characteristics of the dimples utilized to design the tool in this work. The dimple size is dependent on its depth and it can be calculated when the depth and the tool vertex angle are known. According to Figure 2, the relationship between the dimple size, depth and vertex angle is written as follows:

$$\tan\left(\frac{\beta}{2}\right) = \frac{a}{2H} \quad (1)$$

where a, H and β are the dimple size, height and vertex angle, respectively. The dimple size and area shown in Table 1 were calculated using the dimple depth and vertex angle.

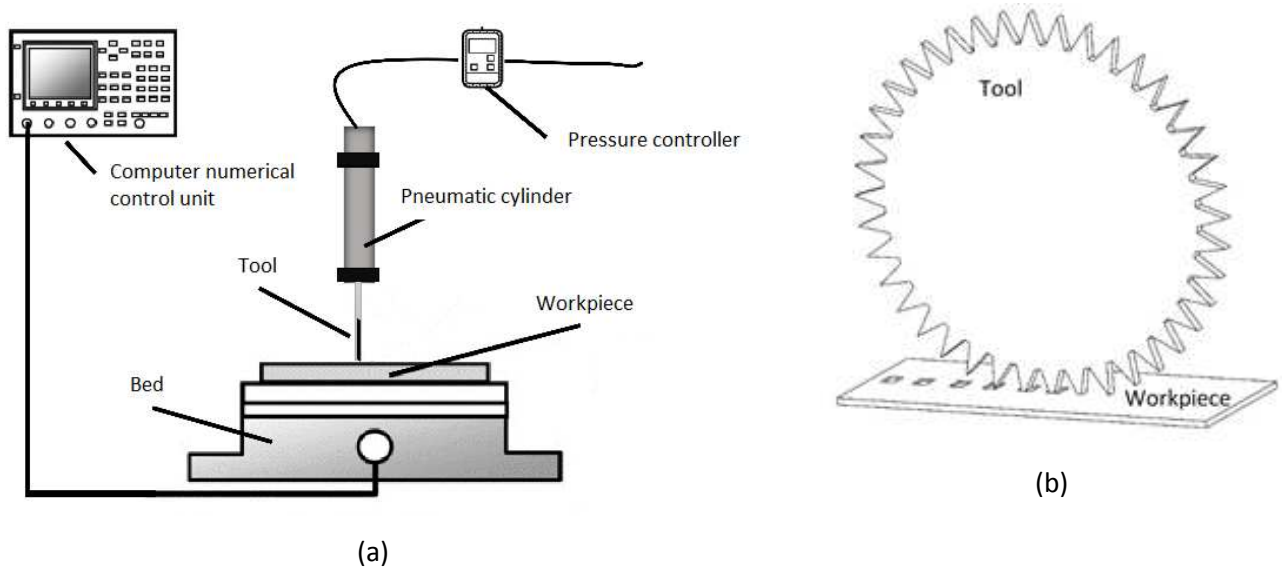

(a) (b)

Figure 1. (a) Schematic of the designed bespoke experimental setup to create dimples using a (b) specific forming tool.

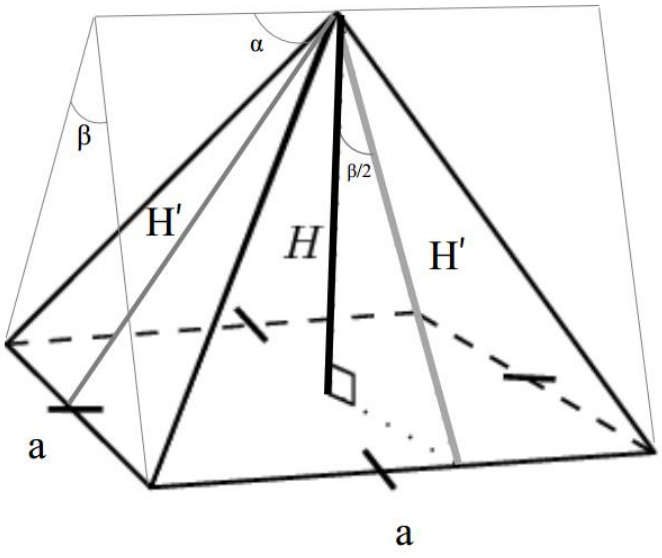

Figure 2. A dimple with square cross-section

Table 1. Characteristics of the dimples used to design the forming

Area density (%)	Depth (µm)	Area (µm^2)	Size (µm)	Cross-section
6	30	31415	177	Square

The designed forming tool was made of DIN 1.2080 alloy steel with hardness of 772 HV, diameter of 40 mm, thickness of 1 mm and 174 teeth. The teeth were cut using a computer numerical control wire-cut machine. Ideally, if the mechanical properties of the surface does not change throughout the surface, the dimple depth remain unchanged as well. A large variation of mechanical properties of the surface results in large deviation of dimples depth. In order to control the dimples depth more accurately, piezoelectric actuators can be used. For the chosen size of dimples in this study, it was observed that the dimple depth did not considerably deviate using the pneumatic cylinder.

2.2. Pin-on-disk apparatus

A set of pin-on disk experiments were used to evaluate the effect of surface textures on friction and wear behaviour. The experiments were performed on a pin-on-disc apparatus where a stationary Mo40 steel pin was pressed against a rotating disc made out of St-37 structural steel. The applied compressive and tangential forces as well as the disk weight loss were measured during the experiments in order to calculate the friction coefficient and the wear resistance of the disk material, respectively.

In order to observe the effects of the generated textures by the micro-dimple rolling apparatus on friction and wear resistance, several discs were prepared using St37 structural steel with diameter of 50 mm and hardness of 220 HV. The pins were also made of Mo40 alloy steel with diameter of 15 mm and hardness of 270 HV. All pins and discs were ground and polished to a surface roughness of Ra=0.32 µm before surface texturing. The discs were then textured using the deformation-based system.

The tests were stopped after relative distance of about 250 m. The specimens were placed into an acetone bath before and after the pin-on-disc tests. The tests were conducted at relative sliding velocities of 0.1 m/s and 0.2 m/s and with the applied normal loads of 25 N and 50 N. The experiments were carried out at dry and lubricated conditions using SAE 10w40 oil as the lubricant.

The standard ball-end pins used for similar experiments have a very small contact area with the disc, reducing the effect of surface texture on the test. Therefore, a flat-end pin with a larger contact area was used instead. A self-adjusting mechanism was also designed to eliminate the effect of misalignment on the test and ensure a complete contact between the sliding flat pin and the textured surface (TS) of the disk. As shown in Figure 3, a ball joint mechanism was used to allow the flat-end pin rotate and adjust itself with the disc. In fact, if the contact pressure becomes larger on one area of the flat-end pin, it creates a moment about the ball joint centre and rotates the pin to reach equilibrium. Therefore, a uniform contact pressure is applied on the contact surface and the whole surface of flat-end pin touches the disc.

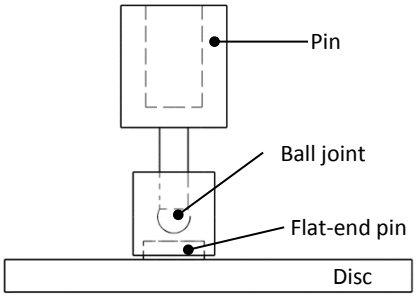

Figure 3. Schematic of the self-adjustment pin-on-disc mechanism.

2.3. Finite element analysis

In order to estimate the required forming load, finite element simulations were run using ABAQUS/Explicit commercial finite element package. Only a small portion of the tool, i.e. five teeth, were modelled in the simulations to save CPU run time. The tool was modelled as a three-dimensional discrete rigid body. The workpiece measures 3500 x 600 x 160 µm and is made of St-37 structural steel. The material response of St-37, as shown in Figure 4, was obtained by uniaxial tensile test. A side view of the assembly is shown in Figure 5. The interaction between the workpiece and the tool was defined through a surface-to-surface contact formulation. The friction was enforced using penalty method with a constant Coulomb friction coefficient of 0.1. The boundary conditions were imposed in two consecutive steps. During the first step, the workpiece bottom surface was fixed and the tool was displaced 30 µm towards the workpiece until the first tooth penetrated into the workpiece. In the second step, a displacement boundary condition was applied at the workpiece bottom surface to move

the workpiece, while the tool's reference point was fixed in all directions except for the rotation around its axis. The 8-noded brick elements in reduced integration mode, denoted by C3D8R in ABAQUS, and a mesh size of 30 µm were used to mesh the workpiece. The rigid tool meshed using rigid 4-noded elements, denoted by R3D4 in ABAQUS, with approximate size of 35 µm as shown in Figure 6.

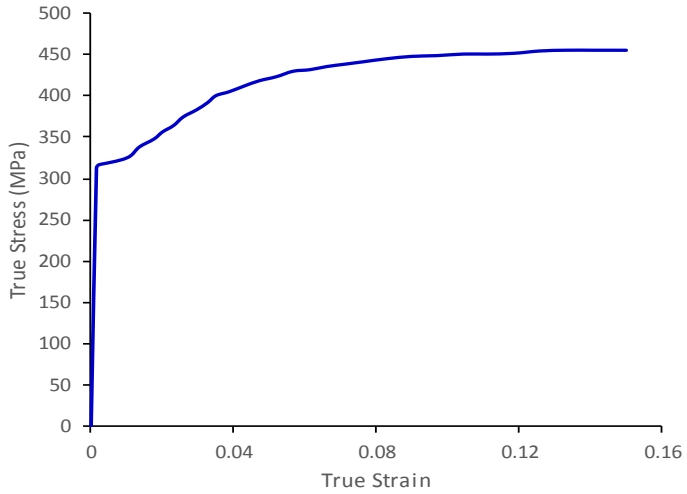

Figure 4. Stress-strain response of St-37 steel in uniaxial tensile test.

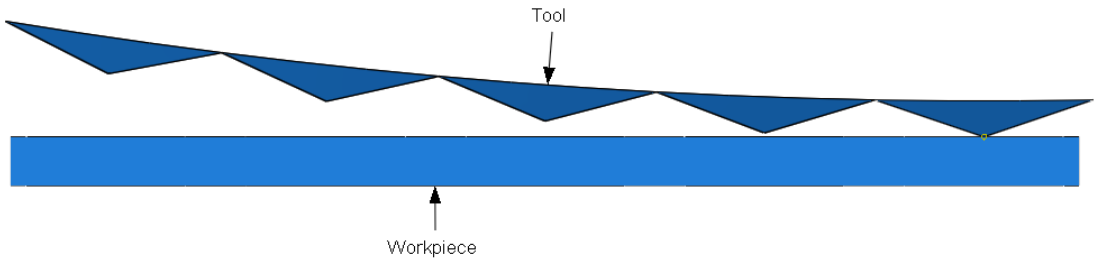

Figure 5. Side view of the assembly.

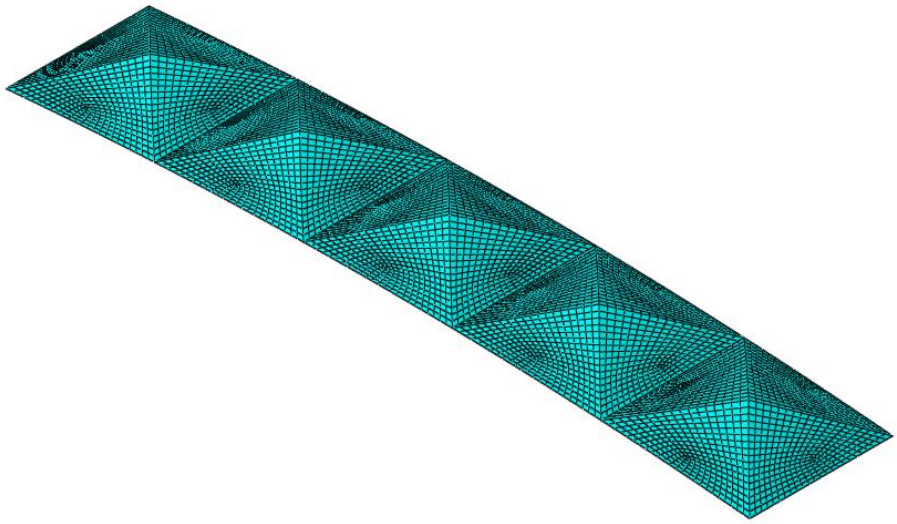

Figure 6. Isometric view of the meshed tool.

3. Results and discussions

Figure 7 shows the distribution of equivalent plastic strain on the final deformed shape of the workpiece. The predicted forming load by finite element was extracted from the simulation results and the required pressure for the load actuator was calculated. The results showed that a pressure of 2.5 bar was required to form dimples of 30 µm on St-37 steel. This pressure was set on the pneumatic actuator utilized to provide the forming load for the tool. It will be shown later in this section that the dimples size and depth predicted by the finite element simulation correlates well with the corresponding experimental dimensions.

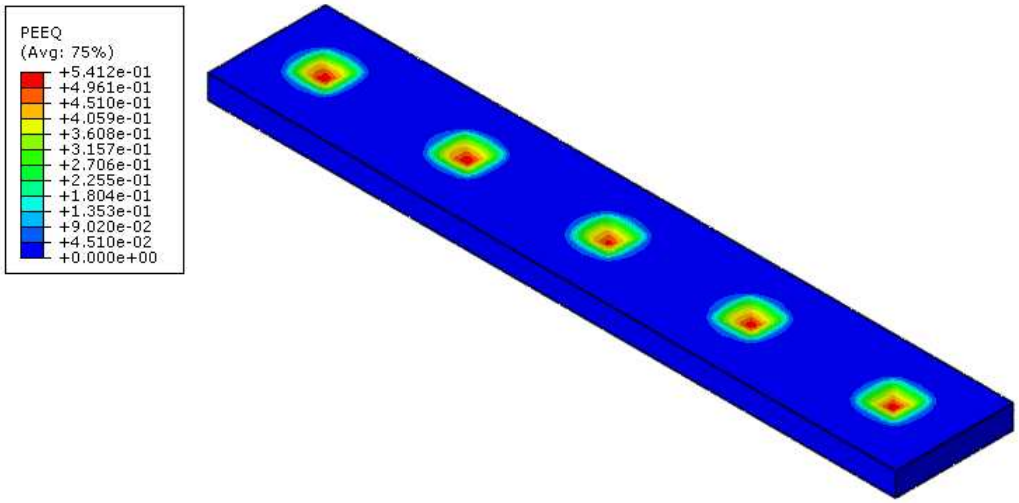

Figure 7. The equivalent plastic strain contour on the final deformed shape of the workpiece.

The TS samples were analysed using optical and scanning electron microscopes (SEM) in order to determine the size of the dimples and the possible mechanisms of deformation within the material. Figures 8a and 8b show the dimples at low and high magnifications where the formation of bumps around the free edges of the dimples makes it difficult to quantify the cross-section of the generated dimples. The discs were polished after the texturing process until the bumps were removed. The dimples on the textured-polished surface (TPS) samples were again observed using the optical microscope as shown in Figures 8c and 8d. The size of six randomly selected dimples were approximately measured, before and after polishing, using optical microscopy images. Figure 9 shows the measured dimples sizes for the surface before and after removing the surface bumps showing a minimal change in the measured values. The high magnification SEM micrographs of the dimples, Figure 10, indicates that the material has been pushed away from the dimple to form the burr along the longitudinal and transverse side of the dimples. Additionally, Figure 11 shows that according to the presence of large shear bands within the dimples, the material has experienced a large shear/compressive deformation during the process. This may results in severe slip bands formation within the grain at the direct vicinity of the surface.

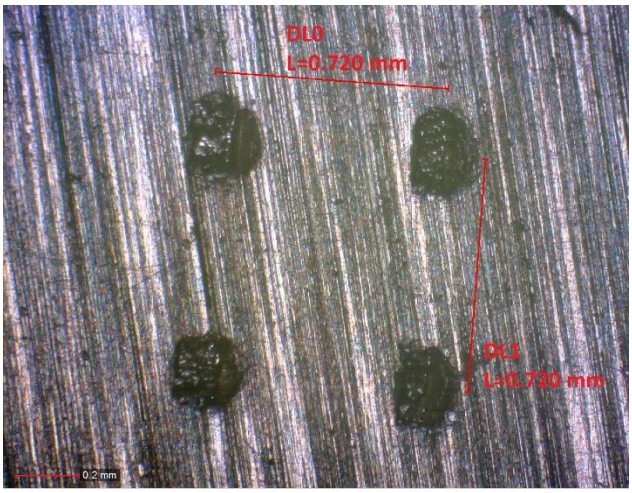

(a)

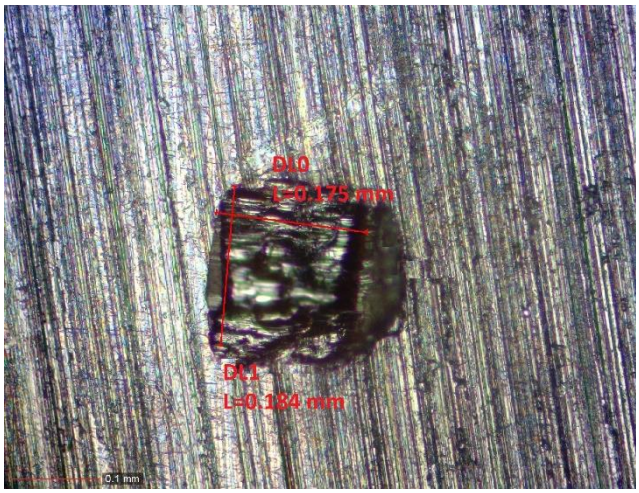

(b)

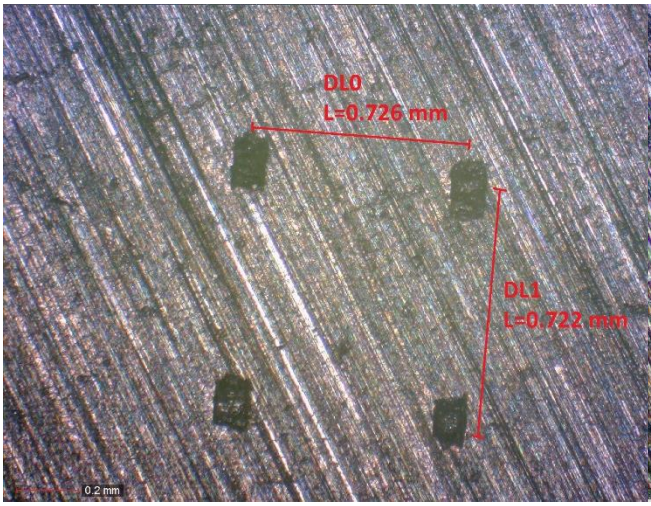

(c)

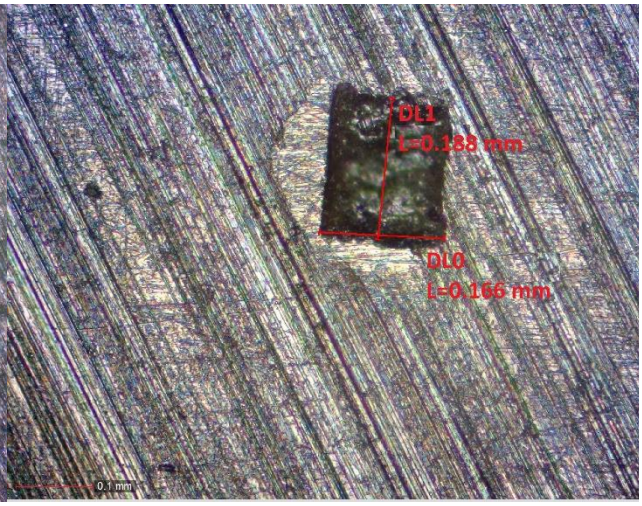

(d)

Figure 8. Optical images of dimples (a,b) before polishing and (c,d) after polishing and removing the surface bumps at low (250X) and high (600x) magnifications (L denotes the measured length and DL0 and DL1 refer to the horizontal and vertical distances, respectively).

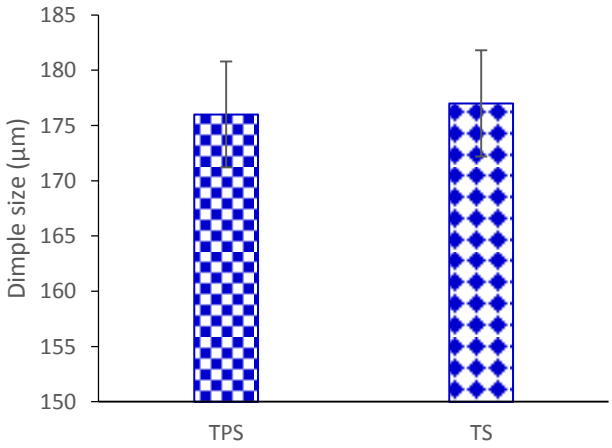

Figure 9. Measured dimples sizes for TS and TPS samples with the calculated standard deviation of 9.6 and 9.3 µm, respectively.

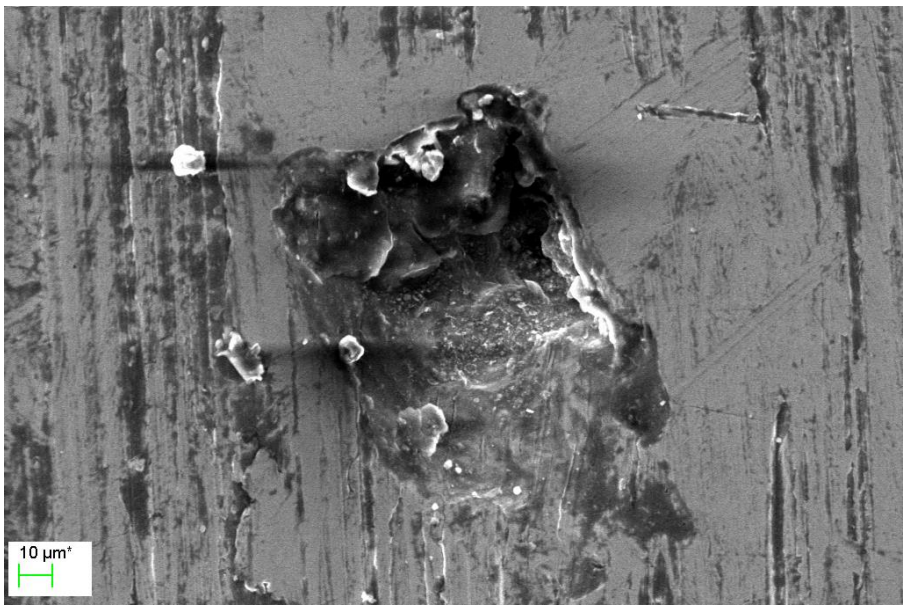

Figure 10. SEM micrograph of a dimple after polishing at magnification of 1000X.

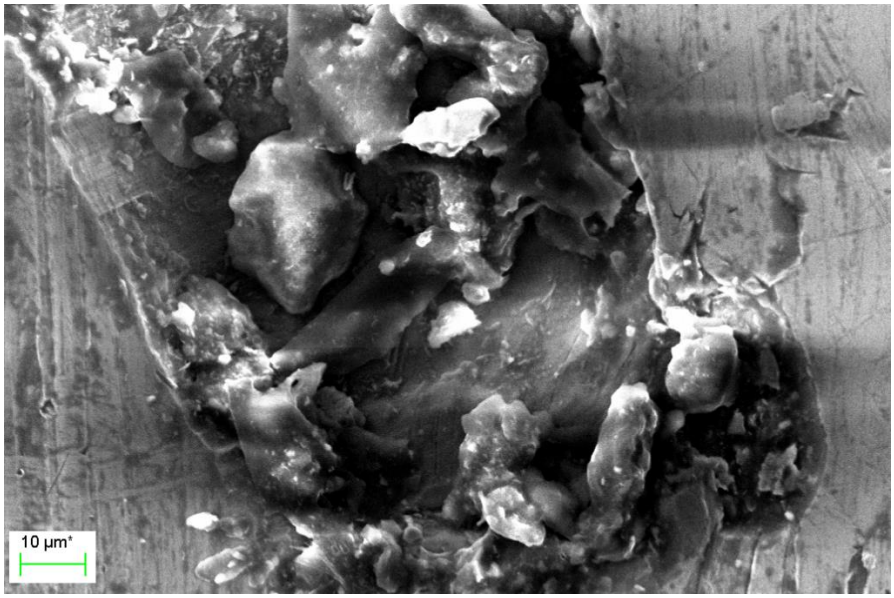

Figure 11. SEM micrograph of a dimple after polishing at magnification of 2000X.

The depth of the formed dimples were measured using a surface profilometer (Mitutoyo-SJ.210 model) and an average depth of about 29.8 µm (with standard deviation of 0.4 µm) was obtained for the dimples. The obtained measurement is in close correlation with the predicted results by the finite element model (30 µm) which indicates the validity of the simulation outputs. Figures 12a and 12b show the surface profile of one dimple before and after the polishing process. The predicted surface profile by finite element simulation was also compared with the experimental one for two consecutive dimples in Figure 13. This figure shows that the predicted profile correlates fairly with the measured profile. The presence of the bumps is also evident in the graphs of Figures 12a and 13.

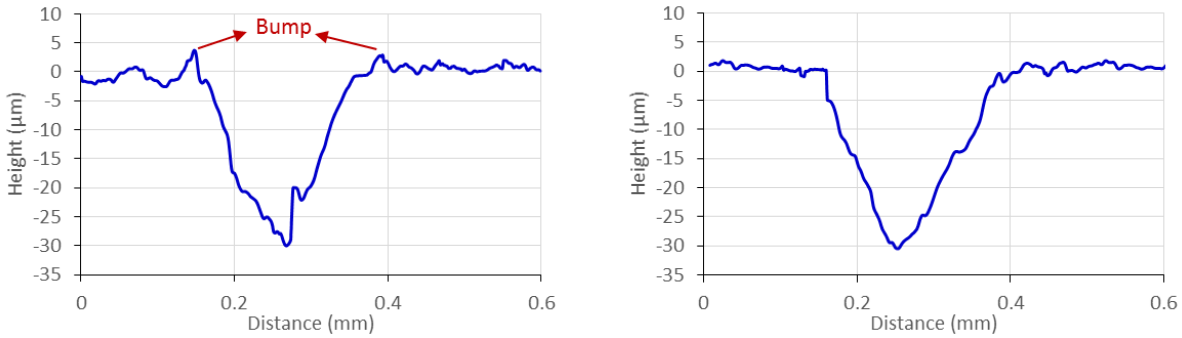

(a) (b)

Figure 12. The surface profile of dimples: (a) before polish and (b) after polish.

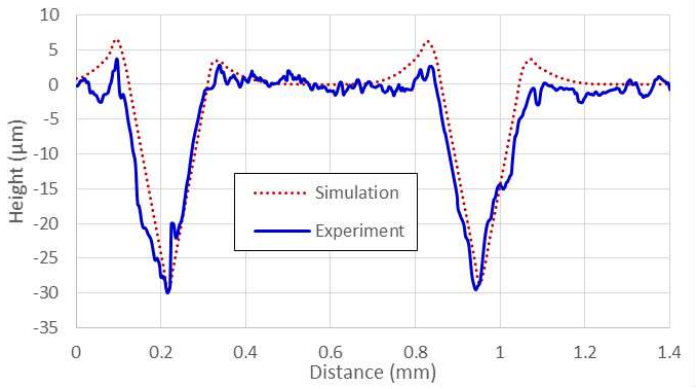

Figure 13. Comparison of the experimentally measured profile with the profile predicted by finite element simulation for two consecutive dimples.

In order to study the effect of bump formation on friction and wear, three types of specimens were prepared: a) without dimples, b) with dimples but without subsequent polishing and c) with dimples and subsequent polishing. The pin-on-disc tests were run at relative sliding velocity of 0.2 m/s and normal load of 50 N. The surface of the discs smeared with SAE 10w40 oil before the tests. The average friction coefficient during the total time of the test was calculated. The effect of subsequent polishing process on friction coefficient and wear is shown in Figures 14 and 15. Figure 14 shows that the friction decrease for the TS and TPS is 0.6% and 4%, respectively. Surprisingly, the mass of material loss for the TS was 70% more than that of the UTS. However, the material loss of about 30% was observed for the TPS compared with the UTS. The bumps start to wear rapidly at the beginning of the test for the TS sample without polishing and more mass is therefore lost during the test. As shown in Figure 16, the friction coefficient is relatively high at the beginning of test. As the test continues, it starts to decrease and eventually saturates to a constant value. This is because of the fact that the asperities formed by bumps increase the coefficient of friction at the beginning of test. However, the friction coefficient stabilizes as the bumps are flattened and it finally becomes smaller than that of the UTS.

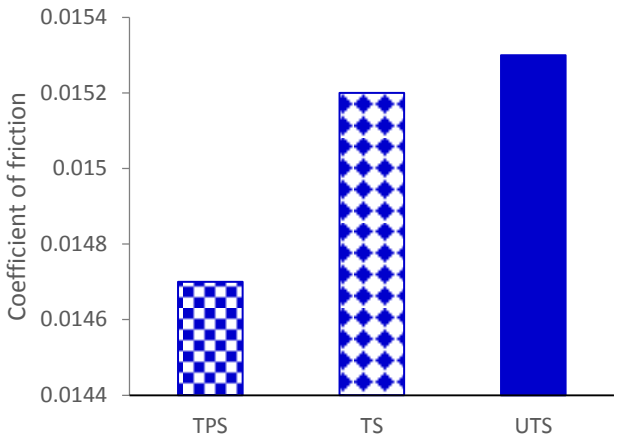

Figure 14. The effect of subsequent polishing on the coefficient of friction.

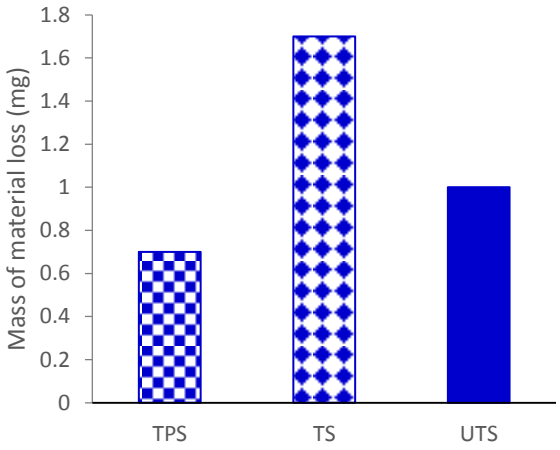

Figure 15. The effect of subsequent polishing on wear.

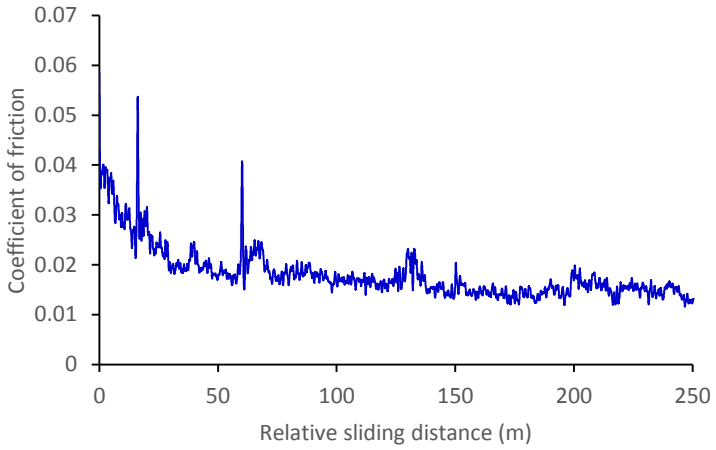

Figure 16. The coefficient of friction for TS without polish during the test.

Figure 17 compares the coefficient of friction for the TPS and UTS in the dry contact condition. The reduction in coefficient of friction is observed for all TPS samples. The figure shows that surface texturing reduces the friction coefficient from 6% to 19% depending on the normal load and velocity. This is because the contact area in TPS is smaller than that of the UTS. The mass of material loss is also compared in Figure 18 for the TPS and UTS. The figure shows that surface texturing reduces the mass loss from 22% up to 32% depending on the applied normal load and sliding velocity. The smaller contact area and trap of wear debris are the main reasons for wear rate reduction of TPS.

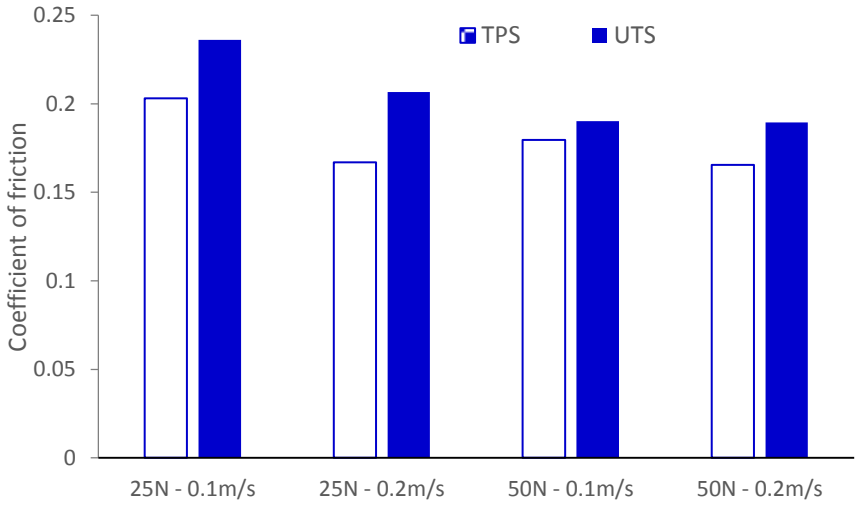

Figure 17. The effect of surface texture on friction in dry condition.

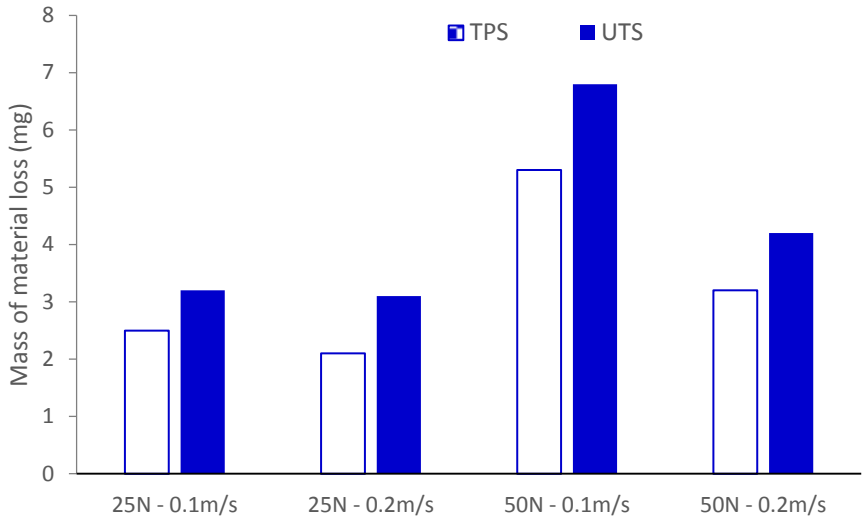

Figure 18. The effect of surface texture on wear in dry condition.

One of the main functions of dimples is to reserve the oil and lubricate the surfaces during contact. In order to study the effect of texturing on friction and wear for lubricated conditions, both the UTS and TPS discs were lubricated by smearing the SAE 10w40 oil before the tests. The coefficient of friction for the TPS and UTS samples are compared in Figure 19. The friction reduction for the TPS in comparison with UTS is from 4% to 23% depending on the normal load and relative sliding velocity. The mass of material loss is also compared in Figure 20 for the TPS and UTS. Compared to the UTS, the mass loss decreases by 30% to 50% for the TPS depending on the normal load and relative sliding velocity. In general, the results show that the dimples reduce both friction and wear by acting as oil pockets and more efficient lubrication of contacting surfaces. In addition, as it can be seen from Figure 19, the friction reduces at larger loads and higher velocities for both UTS and TPS. This is because the pressure increases in the lubricant at larger normal loads and higher sliding velocities which results in formation of a thicker film of lubricant. When the lubricant film is thick enough to maintain hydrodynamic lubrication for the UTS, the dimples do not considerably reduce the friction coefficient for the TPS (4% at normal load of 50 N and velocity of 0.2 m/s). However, as shown in Figure 20, the role of dimples on wear rate reduction is still considerable at larger normal loads and higher velocities. This is because the dimples collect some of the wear debris and reduce the chance of scratching the surfaces. A comparison between the percent of mass loss reduction of TPS in dry and lubricated condition reveals that a larger

decrease is observed when surface texturing is used in lubricated condition where the dimples act both as an oil reservoir and as a micro-trap for wear debris.

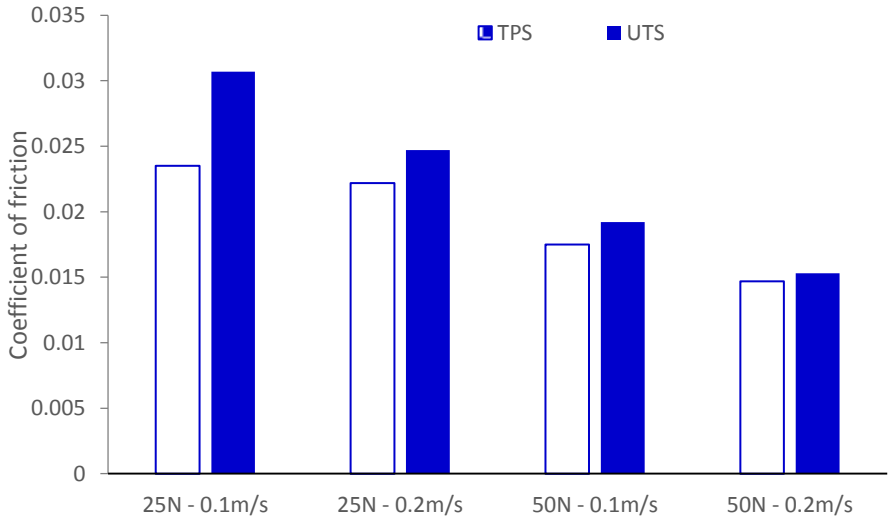

Figure 19. The effect of surface texture on friction in lubricated condition.

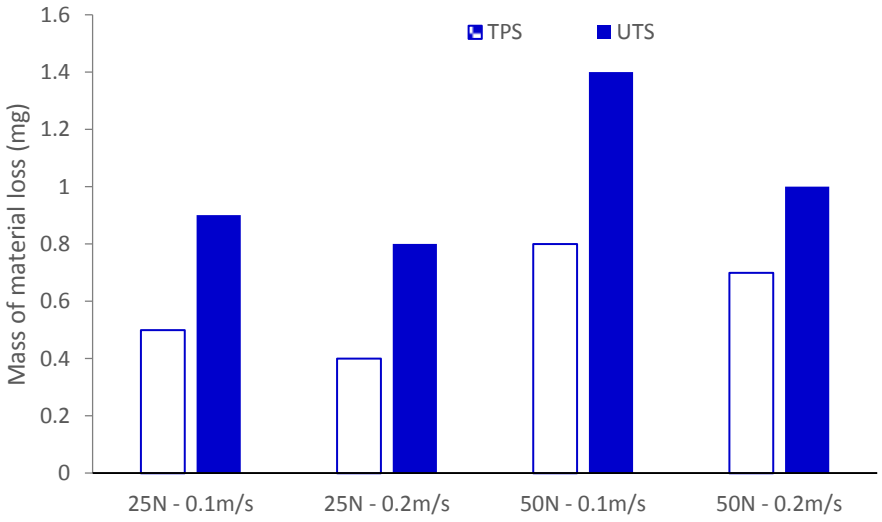

Figure 20. The effect of surface texture on wear in lubricated condition.

Finally, it is worth mentioning that the proposed rolling tool can form hundreds of dimples in less than a minute. It is obvious that more than one tool can also be mounted on a shaft to generate more than one row of dimples with a single travel of the tool and even further reduce the cycle time. The depth of dimple can also be adjusted by changing the force of actuator. However, a new tool must be designed and manufactured for dimples of different shapes and/or different area densities. Therefore, in terms of flexibility, the proposed mechanism may not be able to compete with other texturing methods such as laser ablation process. The application of the proposed mechanism is also limited to the ductile metals with good formability at room temperature.

4. Conclusion

In this study, a rolling tool mechanism was developed to quickly generate micro-dimples on the surface of metals. The system was used to texture the surface of St-37 steel discs. The discs were used in a pin-on-disc apparatus to show that the generated texture could effectively change the frictional and tribological behaviour of the surface. In summary the following conclusions can be drawn:

- Square dimples with sides of approximately 175 μm and depth of 30 μm can be generated on the surface of structural steel.
- The micro-dimples generated by the proposed mechanism are effective to reduce friction and wear both in dry and lubricated contact conditions.
- The system is able to generate hundreds of dimples in less than a minute.
- The bumps formed around the dimples have a negative impact on wear and friction and should be removed to enhance the tribological characteristics of the surface

References

1. Nakada M (1994) Special Issue Tribology for Automobiles in Japan Trends in engine technology and tribology. Tribology International 27 (1):3-8. doi:http://dx.doi.org/10.1016/0301-679X(94)90056-6
2. Hamilton DB, Walowit JA, Allen CM (1966) A Theory of Lubrication by Microirregularities. Journal of Basic Engineering 88 (1):177-185. doi:10.1115/1.3645799
3. Mezghani S, Demirci I, Zahouani H, El Mansori M (2012) The effect of groove texture patterns on piston-ring pack friction. Precision Engineering 36 (2):210-217. doi:http://dx.doi.org/10.1016/j.precisioneng.2011.09.008
4. Zavos AB, Nikolakopoulos PG (2015) Simulation of piston ring tribology with surface texturing for internal combustion engines. Lubrication Science 27 (3):151-176. doi:10.1002/ls.1261
5. Brizmer V, Kligerman Y (2012) A Laser Surface Textured Journal Bearing. Journal of Tribology 134 (3):031702-031702. doi:10.1115/1.4006511

6. Sinanoğlu C, Nair F, Karamış MB (2005) Effects of shaft surface texture on journal bearing pressure distribution. Journal of Materials Processing Technology 168 (2):344-353. doi:http://dx.doi.org/10.1016/j.jmatprotec.2005.02.252
7. Wang X, Kato K, Adachi K, Aizawa K (2003) Loads carrying capacity map for the surface texture design of SiC thrust bearing sliding in water. Tribology International 36 (3):189-197. doi:http://dx.doi.org/10.1016/S0301-679X(02)00145-7
8. Sharma N, Kango S, Tayal A, Sharma RK, Sunil (2016) Investigations on the Influence of Surface Texturing on a Couple Stress Fluid–Based Journal Bearing by Using JFO Boundary Conditions. Tribology Transactions 59 (3):579-584. doi:10.1080/10402004.2015.1094840
9. Grabon W, Koszela W, Pawlus P, Ochwat S (2013) Improving tribological behaviour of piston ring–cylinder liner frictional pair by liner surface texturing. Tribology International 61:102-108. doi:http://dx.doi.org/10.1016/j.triboint.2012.11.027
10. Zhou Y, Zhu H, Tang W, Ma C, Zhang W (2012) Development of the theoretical model for the optimal design of surface texturing on cylinder liner. Tribology International 52:1-6. doi:http://dx.doi.org/10.1016/j.triboint.2011.12.017
11. Etsion I, Kligerman Y, Halperin G (1999) Analytical and Experimental Investigation of Laser-Textured Mechanical Seal Faces. Tribology Transactions 42 (3):511-516. doi:10.1080/10402009908982248
12. Ahmed A, Masjuki HH, Varman M, Kalam MA, Habibullah M, Al Mahmud KAH (2016) An overview of geometrical parameters of surface texturing for piston/cylinder assembly and mechanical seals. Meccanica 51 (1):9-23. doi:10.1007/s11012-015-0180-6
13. Wang X, Giovannini M, Xing Y, Kang M, Ehmann K (2015) Fabrication and tribological behaviors of corner-cube-like dimple arrays produced by laser surface texturing on medical needles. Tribology International 92:553-558. doi:http://dx.doi.org/10.1016/j.triboint.2015.07.042
14. Pettersson U, Jacobson S (2003) Influence of surface texture on boundary lubricated sliding contacts. Tribology International 36 (11):857-864. doi:http://dx.doi.org/10.1016/S0301-679X(03)00104-X
15. Etsion I (2013) Modeling of surface texturing in hydrodynamic lubrication. Friction 1 (3):195-209. doi:10.1007/s40544-013-0018-y
16. Zhou R, Cao J, Ehmann K, Xu C (2011) An Investigation On Deformation-Based Surface Texturing. Journal of Manufacturing Science and Engineering 133:061017-061011
17. Ranjan R, Lambeth DN, Tromel M, Goglia P, Li Y (1991) Laser texturing for low-flying-height media. Journal of Applied Physics 69 (8):5745-5747. doi:doi:http://dx.doi.org/10.1063/1.347908
18. Christian G, Tobias M, Daniel B, Andrea C, Franco M (2015) Optimum dimple diameter for friction reduction with laser surface texturing: the effect of velocity gradient. Surface Topography: Metrology and Properties 3 (4):044001
19. Kovalchenko A, Ajayi O, Erdemir A, Fenske G, Etsion I (2005) The effect of laser surface texturing on transitions in lubrication regimes during unidirectional sliding contact. Tribology International 38 (3):219-225. doi:http://dx.doi.org/10.1016/j.triboint.2004.08.004
20. Ryk G, Kligerman Y, Etsion I (2002) Experimental Investigation of Laser Surface Texturing for Reciprocating Automotive Components. Tribology Transactions 45 (4):444-449. doi:10.1080/10402000208982572
21. Etsion I (2004) Improving Tribological Performance of Mechanical Components by Laser Surface Texturing. Tribology Letters 17 (4):733-737. doi:10.1007/s11249-004-8081-1
22. Shin HS, Park MS, Chu CN (2010) Electrochemical etching using laser masking for multilayered structures on stainless steel. CIRP Annals - Manufacturing Technology 59 (1):585-588. doi:http://dx.doi.org/10.1016/j.cirp.2010.03.134
23. Zhang J, Meng Y (2012) A study of surface texturing of carbon steel by photochemical machining. Journal of Materials Processing Technology 212 (10):2133-2140. doi:http://dx.doi.org/10.1016/j.jmatprotec.2012.05.018

24. Chen X, Qu N, Hou Z (2016) Electrochemical micromachining of micro-dimple arrays on the surface of Ti-6Al-4V with NaNO3 electrolyte. The International Journal of Advanced Manufacturing Technology:1-10. doi:10.1007/s00170-016-8807-x
25. Zhu D, Qu NS, Li HS, Zeng YB, Li DL, Qian SQ (2009) Electrochemical micromachining of microstructures of micro hole and dimple array. CIRP Annals - Manufacturing Technology 58 (1):177-180. doi:http://dx.doi.org/10.1016/j.cirp.2009.03.004
26. Byun JW, Shin HS, Kwon MH, Kim BH, Chu CN (2010) Surface texturing by micro ECM for friction reduction. International Journal of Precision Engineering and Manufacturing 11 (5):747-753. doi:10.1007/s12541-010-0088-y
27. Zhang X, Qu N, Chen X (2016) Sandwich-like electrochemical micromachining of micro-dimples. Surface and Coatings Technology 302:438-447. doi:http://dx.doi.org/10.1016/j.surfcoat.2016.05.088
28. Guo P, Ehmann KF (2013) Development of a tertiary motion generator for elliptical vibration texturing. Precision Engineering 37 (2):364-371. doi:http://dx.doi.org/10.1016/j.precisioneng.2012.10.005
29. Guo P, Lu Y, Pei P, Ehmann KF (2014) Fast Generation of Micro-Channels on Cylindrical Surfaces by Elliptical Vibration Texturing. Journal of Manufacturing Science and Engineering 136 (4):041008-041008. doi:10.1115/1.4027126
30. Shen X, Zhang J (2013) Studies on friction and wear properties of surface produced by ultrasonic vibration-assisted milling. The International Journal of Advanced Manufacturing Technology 67 (1):349-356. doi:10.1007/s00170-012-4488-2
31. Wang X, Kato K (2003) Improving the Anti-seizure Ability of SiC Seal in Water with RIE Texturing. Tribology Letters 14 (4):275-280. doi:10.1023/A:1022650813314
32. Amanov A, Cho IS, Pyoun YS, Lee CS, Park IG (2012) Micro-dimpled surface by ultrasonic nanocrystal surface modification and its tribological effects. Wear 286–287:136-144. doi:http://dx.doi.org/10.1016/j.wear.2011.06.001
33. Su X, Shi L, Huang W, Wang X (2016) A multi-phase micro-abrasive jet machining technique for the surface texturing of mechanical seals. The International Journal of Advanced Manufacturing Technology:1-8. doi:10.1007/s00170-015-8272-y
34. Stephens LS, Siripuram R, Hayden M, McCartt B (2004) Deterministic Micro Asperities on Bearings and Seals Using a Modified LIGA Process. Journal of Engineering for Gas Turbines and Power 126 (1):147-154. doi:10.1115/1.1619430
35. FUTAMURA M, DOHDA K, MAKINO T, SUZUKI T (2009) Development of Micro-Dimple Forming for Inner Surface of Pipe. Journal of the Japan Society for Technology of Plasticity 50 (580):434-438. doi:http://doi.org/10.9773/sosei.50.434
36. Zhou R, Cao J, Ehmann K, Chuang Y, Lee A, Wu C, Huang K A novel desktop deformation based micro surface texturing system. In, 2011.
37. Cao J, Dohda K, Zhou R, Makino T, Futamura M (2010) An Investigation on Bump Formation in Forming of Micro Dimples. Steel Research International 81:1160-1165